Observation of orbital ordering and Jahn-Teller distortions supporting the Wigner-crystal model in highly doped Bi$_{1-x}$Ca$_x$MnO$_3$

S. Grenier

Physics Department, Brookhaven National Laboratory, Upton, New York 11973, USA
and Institut Néel, C.N.R.S., 25 Avenue des Martyrs, BP 166, 38042, Grenoble cedex, France

V. Kiryukhin, S-W. Cheong, and B. G. Kim

Department of Physics and Astronomy, Rutgers University, Piscataway, New Jersey 08854, USA

J. P. Hill and K. J. Thomas

Physics Department, Brookhaven National Laboratory, Upton, New York 11973, USA

J. M. Tonnerre and Y. Joly

Institut Néel, C.N.R.S., 25 Avenue des Martyrs, BP 166, 38042, Grenoble cedex, France

U. Staub and V. Scagnoli

Swiss Light Source, Paul Sherrer Institute, 5232 Villigen, Switzerland

We report on the experimental characterization of orbital ordering and the associated lattice distortions in highly doped Bi$_{1-x}$Ca$_x$MnO$_3$. Resonant x-ray diffraction was used at the Mn L-edge for the direct observation of the ordered localized states, and at the Mn K-edge for the sensitivity to the distortions of the manganese-oxygen octahedra. The orbital ordering on Mn atoms was directly observed at $x=0.69$; the analysis and the numerical simulations of the K-edge spectra allow us to characterize the pattern of the distorted octahedra at $x=\frac{4}{5}$. These observations support the Wigner-crystal-type model at both dopings; the bi-stripe model is ruled out at $x=0.69$.

I. INTRODUCTION

Crystallization of charge carriers in doped transition-metal oxides may exhibit charge and orbital orderings. As the insulating phase competes with metallic ferromagnetism or superconductivity, it is essential to determine precisely which electronic orderings take place to help identify the correlations that induce the phase transitions and stabilize each state. However, the characterization of an electronic crystal remains an experimental challenge. Conventional crystallography is difficult as charge and orbital orderings correspond to a small spatial variation of the electronic density with a weak scattering amplitude for x-rays or electrons. For example, orbital ordering of the $3d^4$ configuration in x hole-doped manganites concerns $1-x$ electron per chemical unit. In fact, recent neutron, x-ray, and electron crystallographic studies have shown that it is also a strenuous task to determine the space group and the amplitudes of the atomic displacements related to the electronic phase transitions.[1,2]

Experimental efforts aimed at directly detecting periodic electronic structures relevant to transport and magnetism are undertaken utilizing complementary techniques. In the past few years, resonant x-ray diffraction (RXD) has been invaluable in the characterization of charge and orbital ordering. This technique combines crystallographic and spectroscopic information, exploiting its sensitivity to crystallographic sites, chemical elements, and spectral density of states, as illustrated in the following. In this paper we address the experimental characterization of the periodic electronic con-figuration on Mn atoms in manganites within complex (large) unit cells, at high doping, thereby distinguishing between two models recently proposed. In previous studies, it was shown that at half-doping a Wigner-crystal (WC) model describes the electronic organization on the Mn atoms.[3] At higher doping the WC model was also proposed along another model, the so-called "bi-stripe" model.[4] Here, the use of RXD provides direct evidence of orbital ordering on the $3d$-like band in Bi$_{1-x}$Ca$_x$MnO$_3$ ($x=0.69$) with a pattern of electronically equivalent Mn atoms corresponding to a WC model. We show that an alternative model based on a bi-stripe organization of equivalent Mn atoms can be ruled out. The WC model is also strongly supported at higher doping $\left(x=\frac{4}{5}\right)$. We show that several RXD spectra are satisfyingly reproduced with a crystallographic model based on the displacement patterns observed in a smaller WC unit cell $\left(x=\frac{2}{3}\right)$.

II. METHODS

Resonant x-ray diffraction was performed at the L_{III}- and L_{II}-edges and at the K-edge of the Mn atoms. These edges correspond to the momentary ($\Gamma \sim 10^{-15}$ s) transition of a $2p$ electron to an unoccupied $3d$ orbital, and of a $1s$ electron to an unoccupied $4p$ orbital, respectively. The transition is induced by the absorption followed by the reemission of a photon with the energy that separates the excited states from the ground state. By sweeping the incident photon energy

through the edges, the spectrum of the density of unoccupied states is probed, the spectrum being weighted by the crystallographic structure factor. So, these energy scans modulate the amplitude of the scattering factor of the resonant atoms, and therefore the intensity of the diffraction peaks.

With the diffraction vector chosen to correspond to the propagation vector of some periodic electronic features, these resonances provide two sensitivities relevant to the present study. The first technique is sensitive to the spectrum of the ordered states that are active in the physical properties of the system. Specifically, it allows the observation of the orbital ordering in manganite. It is achieved at the Mn $L_{II/III}$-edges as it directly probes the first unoccupied states that derive from the atomic Mn $3d$,[5–10] these states being hybridized Mn $3d$ and O $2p$ states. For the present study, L-edge data were collected at the SIM beamline of the Swiss Light Source using the RESOXS ultrahigh vacuum chamber.[11,10] The energy resolution was about 300 meV. The σ or π incident polarizations (perpendicular to and within the scattering plane, respectively) were chosen thanks to two Apple undulators.

The second technique utilizes the Mn K-edge and is sensitive to the $4p$ and higher p states, about 10 eV above the Fermi level. While these states are neither active in determining the physical properties, nor reflecting significantly the active states, they do depend strongly on the surrounding atomic configuration due to band structure effects.[5,12,13,5,14–16] One can therefore take advantage of the difference in the spectrum of p states on Mn atoms that sit in different surrounding structures. At the $1s \rightarrow 4p$ resonance, this difference can result in a scattering contrast equivalent to $\sim$5 electrons for Mn atoms sitting in different crystallographic sites,[16] be the difference in the electronic density as small as one-tenth of an electron. The maximum contrast is realized when inequivalent atoms scatter with opposite phase, if their distance is at least $1/4$ of the wavelength λ. In principle the sensitivity to the different crystallographic sites can be exploited at either the L-edges or the K-edge. However, λ is about 19 Å at the L-edges; the available reciprocal space is reduced to typically one reflection only. The short wavelength at the K-edge ($\lambda \sim 2$ Å) allows several Bragg reflections and the maximum contrast between inequivalent sites can be realized. As shown below, the K-edge spectra measured on superstructure reflections that are weak off-resonance are extremely sensitive to the subtle displacements of *all* the atoms of the unit cell as a result of the interference of the resonant contrast (strong on superstructure peak) with Thomson scattering (very weak but information rich). K-edge data were taken at the X22C beamline of the National Synchrotron Light Source (Brookhaven National Laboratory). A Ge(111) monochromator was used providing an energy resolution of 3 eV. The incident polarization was σ.

In order to help interpret the K-edge resonant spectra, numerical simulations of the data were performed with the FDMNES code.[17] This program calculates the density of states in a monoelectronic approximation within the full multiple scattering formalism and calculates the matrix elements between the core electronic state $1s^2 4p^0$ and the excited states $1s^1 4p^1$. Because the main signal measured at the K-edge cor-

responds to rather delocalized states, 10 eV above the Fermi level, the calculations are performed without consideration of any particular $3d$ distribution.[12] In fact, we adopt a monoelectronic formalism where correlations are treated by a Hedin-Lundquist potential. No calculations of the L-edges spectra were attempted. The calculation of both the ground state and the excited states involving the strongly correlated $3d$ band is beyond the scope of the present paper; dedicated studies have been presented recently.[6,9,18] In this paper, qualitative, yet definitive, conclusions have been drawn on the pattern of the orbital ordering, but not at the quantitative level for the electronic structure itself.

In principle RXD is also sensitive to charge ordering, that is to differing net electronic densities on different Mn sites. This sensitivity comes from the shift of the core level energies due to different screening by the electronic densities, and from different densities of the unoccupied states. In mixed-valent oxides, the measured difference in density is much smaller than the formal valence. Nazarenko *et al.*[19] and Joly *et al.*[20] have recently evaluated the charge density segregation in Fe_3O_4 and NaV_2O_5. They found 0.12 and 0.04 electrons, respectively, from a first-principles fit to the experimental data (instead of one electron). Herrero-Martin *et al.*[21] explored an empirical method and claimed a segregation of $\pm 0.08 e^-$ in charge-ordered manganites. In fact, most of the K-edge signal is due to modulations of the $4p$ states whereas at the L-edge the charge ordering wave vector is not accessible for the systems studied. Therefore in the present study we do not consider further the charge ordering.

Here we report results in the $Bi_{1-x}Ca_xMnO_3$ system with two high dopings, $x=0.69$ and 0.8. These systems have an electronic phase transition at $T=220$ and 165 K, respectively. The transitions have been interpreted as a charge and orbital ordering on different types of Mn atoms, with significant difference in the orbital occupancies, following a pattern in the unit cell that has yet to be characterized. The same phase transitions have been studied mostly in the $La_{1-x}Ca_xMnO_3$ system. However, to the best of our knowledge, no single crystal has been grown for $x \geq 0.5$ preventing thorough RXD studies. In contrast, it is possible to grow highly doped (Bi, Ca) single crystal, allowing us to perform RXD measurements on the weak superstructure reflections with a good counting statistics. Single crystals were grown by the flux technique and characterized by hard x-ray diffraction. When refering to the reflections, we use the *Pbnm* orthorhombic notations for the unit cell above the electronic phase transition.

III. RESULTS

Figure 1 shows the spectra taken at the L_{III}- and L_{II}-edges of the sample $Bi_{0.31}Ca_{0.69}MnO_3$ for the reflection $(0\delta0)$, where $\delta=0.31$. This Q is expected to correspond to the orbital ordering reflection; it is the only superstructure reflection observable at these edges. RXD spectra for two incident polarizations are shown. Because there was no polarization analysis on the scattered photons, the two measurements correspond to $\sigma \rightarrow \sigma + \pi$ and $\pi \rightarrow \sigma + \pi$ channels, the σ polarization is directed along the **a** axis, as shown in Fig. 2. Signifi-
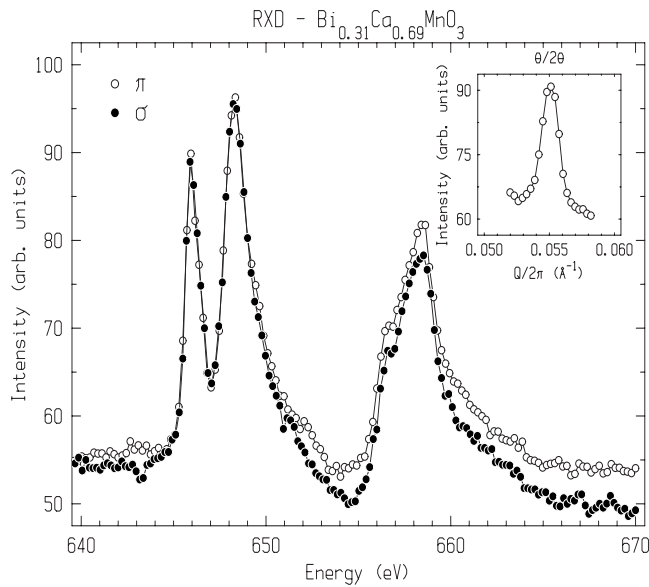
FIG. 1. $L_{II/III}$-edge resonant x-ray diffraction spectra of the $(0\,\delta\,0)$ reflection ($\delta=0.31$) for $Bi_{0.31}Ca_{0.69}MnO_3$, at $T=200$ K taken with two polarizations of the incident photon, π and σ (without absorption correction). Inset, longitudinal Q-scan.

cantly, the two channels have not only the same energy line shape, but also the same intensity all over the L_{III}-edge. The energy line shape is the same also at the L_{II}-edge but we attribute the difference in intensity to a slight misaligment of the optical path along the beamline for the two incident polarizations. In the following, we assume that the two channels give equal scattering. This result leads to the conclusion that the scattering channel is mainly rotated, corresponding to $\sigma\rightarrow\pi$ and $\pi\rightarrow\sigma$, respectively. This is because the $\pi\rightarrow\pi$ channel is weighted by the polarization factor P compared to the $\sigma\rightarrow\sigma$ channel, $P=\cos^2 2\theta_B$. With $\theta_B=32.13°$ at 650 eV, $P\sim19\%$. Moreover, different matrix elements are probed for the $\sigma\rightarrow\sigma$ and $\pi\rightarrow\pi$ channels which should give rise to different energy line shapes in the manganite systems.[16] Instead, the same matrix elements are probed for the two rotated channels.[16] The absence of variation in the line shape and even in the intensity suggests that the two unrotated channels are negligible, and that the scattering is
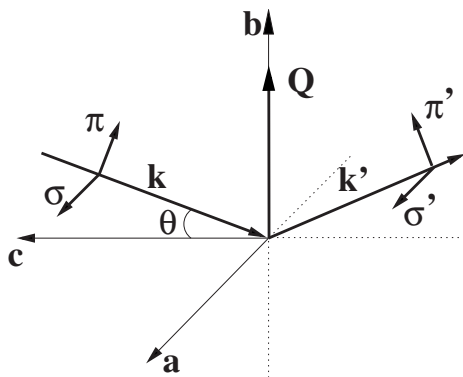

FIG. 2. Scattering geometry for the L-edge experiment. The crystallographic directions of the sample are indicated following the *Pbnm* settings.
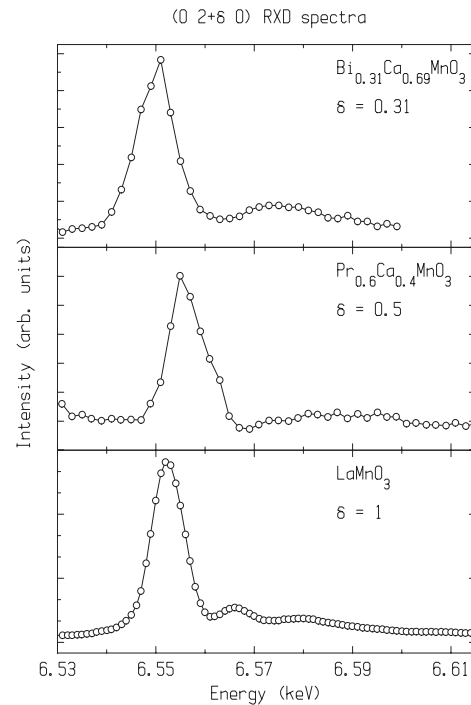

FIG. 3. K-edge resonant x-ray diffraction spectra of the $(0\,2+\delta\,0)$ reflection for various doped manganites in their orbital ordered phase (without self-absorption correction). Similarities in the spectra indicate the presence and the same specific arrangement of Jahn-Teller distorted octahedra. The slight shift (about 2 eV) in the resonance is due to various interatomic distances and differing energy calibrations on the beamline.

purely rotated, that is $\sigma\rightarrow\pi$ and $\pi\rightarrow\sigma$, respectively. These results are consistent with all the resonant measurements performed on the reflections with wave vectors corresponding to the propagation vectors of the orbital ordering.[10,16,22,23] In the discussion, we will conclude that one of the proposed models (the bi-stripe) is ruled out, and that instead the Wigner-Crystal type structure is strongly supported.

Figure 3 shows the K-edge resonant spectra of the $(0\,2+\delta\,0)$ for three manganites at various dopings, including the same $Bi_{0.31}Ca_{0.69}MnO_3$ sample used for the L-edge experiment. This reflection is the first superstructure reflection from the main Bragg reflection $(0\,2\,0)$ (it is the fifth order of the reflection measured at the L-edge). For the three systems, the energy line shapes are similar and the scattering off-resonance, if any, is at least two orders of magnitude smaller than on resonance. For the two other systems, it was found that this reflection corresponds to the propagation vector of oxygen octahedra having the same distortion (Jahn-Teller distortion), and that the scattering was purely rotated ($\sigma\rightarrow\pi$).[16] Here, the incident polarization was σ and no polarization analyzer was used. Similar energy line shapes may be an indication that similar matrix elements of the scattering tensor are probed, and that the scattering channel may also be purely rotated for the $Bi_{0.31}Ca_{0.69}MnO_3$ system, as deduced from the L-edge data.

Figure 4 shows K-edge resonant spectra of main and superstructure reflections for $Bi_{0.2}Ca_{0.8}MnO_3$ in the OO phase. The spectra for $(1\,1+2\delta\,6)$ and $(2\,2+2\delta\,6)$ are strikingly

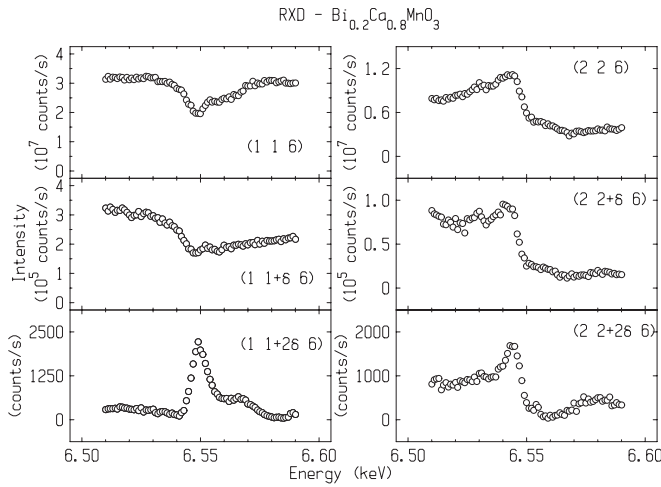FIG. 4. *K*-edge resonant x-ray diffraction spectra for $Bi_{0.2}Ca_{0.8}MnO_3$ in the orbital ordered phase (8.5 K), $\delta \sim 0.20$ (without absorption correction).

reminiscent of all the published spectra interpreted as Jahn-Teller distorted and undistorted octahedra diffracting with opposite crystallographic phase, in half-doped manganites.[14,16] As in those studies, the main scattering channel is $\sigma \rightarrow \sigma$ as deduced from the numerical simulations discussed below. The strong variation in the line shape of the superstructure reflections is a clear indication of the contrast, presumably maximum, realized between crystallographically different Mn sites.

IV. DISCUSSION

The present study is aimed at determining the pattern of the orbital ordering in highly doped manganites and distinguishing between different electronic patterns proposed recently. The analysis relies on the direct probe of the electronic structure of a subset of the Mn atoms, and on the sensitivity to distortions of octahedra associated with the orbital ordering of the (formal) $3d^4$ configuration.

The crystallographic structure of $LaMnO_3$ shows Jahn-Teller distortions of the O octahedra consisting of long and short Mn–O bonds.[24] This peculiar structure is associated with orbital ordering of the $3d^4$ configuration. This ordering has not yet been directly probed experimentally but it is obtained by first-principles calculations.[25,26] As the system is doped, various crystallographic and magnetic structures appear. At half-doping, say for $La_{0.5}Ca_{0.5}MnO_3$, the unit cell is doubled with a checkerboard organization of distorted and undistorted octahedra.[2,3,16] This structure also reflects a recently observed orbital ordering.[7–10] At higher doping, two electronic models were proposed: the "Wigner crystal" and the "bi-stripe" models. The WC model consists of $3d^4$ atoms placed as far apart as possible in the (ab) plane, whereas the bi-stripe model places equivalent Mn closer to each other and forms stripes perpendicular to the orbital ordering direction.[4] These two different patterns of orbital ordering lead to different considerations over the importance of electron-lattice coupling and Coulomb repulsion in defining the physics of the system.

Electron diffraction and high-resolution imaging were first interpreted according to the bi-stripe model,[27] but image simulations showed that the WC model was more likely.[28] The crystallographic structure of $La_{0.33}Ca_{0.66}MnO_3$ was obtained by Radaelli *et al.* using neutron scattering.[4] The refinements reached the lowest minimum with the WC structure "within the limits of the sets of constraints imposed." If the ligand-metal displacements associated with the orbital ordering are clearly detected by crystallography, the standard method only resolves the supercell with great difficulty. Even for the relatively simpler half-doped compound, various crystallographic structures, corresponding to various orbital order patterns, were proposed.[2]

The *L*-edge RXD spectra presented in Fig. 1 can differentiate the two proposed models. At the diffraction vector $(0\ \delta\ 0)$, with $\delta = b/\Lambda$ and Λ the orbital order supercell size along $\boldsymbol{b}$, the atoms separated by $\Lambda/2$ scatter in opposite phase, that is, with the maximum contrast. For the bi-stripe model these atoms are electronically and crystallographically different. This should allow all the scattering channels to occur at the resonance, in particular the $\sigma \rightarrow \sigma$ and $\pi \rightarrow \pi$ scatterings, like for the so-called charge-order reflections observed at half doping.[16] In fact, their electronic structures being different, these Mn atoms can be considered as different x-ray scatterers at the resonance, like two different elements. Instead, our measurements show that the scattering in the $\sigma \rightarrow \sigma$ and $\pi \rightarrow \pi$ channels is forbidden, that the scattering is rotated, of the type $\sigma \rightarrow \pi$. Therefore we find that the atoms are equivalent, electronically and crystallographically. The scattering is only due to the same electronic anisotropy on each equivalent site, exactly as observed and explained in previous orbital ordering studies.[10,16,29] This deduction applies to every couple of Mn atoms of the unit cell separated by $\Lambda/2$: this pattern of equivalent Mn corresponds to the WC model.

There is, however, a limitation in the determination of the whole orbital ordering pattern. Here, the direct observation of orbital ordering occurs only from sites that are Jahn-Teller distorted; it is the anisotropy of the electronic structure of a subset of the Mn atoms that allows the scattering, whereas isotropic electronic structures are "transparent." Therefore the set of data is not complete in order to determine the pattern of the orbital ordering in the whole unit cell, where supposedly undistorted octahedra separate the distorted octahedra. One would need to realize an opposite phase shift between distorted and undistorted octahedra, which is prevented in many manganite systems by the too large wavelength at the *L*-edge.

To conclude on this analysis of the *L*-edge data, we can affirm that the orbital ordering was directly evidenced, that all the Mn atoms separated by $\Lambda/2$ are electronically equivalent, that it contradicts the bi-stripe model, and supports the WC model.

The $(0\ 2 + \delta\ 0)$ RXD spectra presented in Fig. 3 were taken at the *K*-edge. It corresponds to the same propagation vector as the orbital ordering, like before, but with sensitivity to the distortions in the surrounding crystallographic structure of the Mn atoms. The similar energy line shape for the three spectra of the same $(0\ 2 + \delta\ 0)$ reflection calls for the same conclusion drawn in previous studies for undoped and

TABLE I. Atomic positions for a constructed Wigner-crystal model for $Bi_{0.2}Ca_{0.8}MnO_3$, in the *Pbnm* space group, according to displacement directions obtained for $La_{0.33}Ca_{0.66}MnO_3$ (Ref. [4]).

Atoms	x	y	z
Mn_1	0.018	0.1	0
Mn_2	0.018	0.3	0
Mn_3	0	0.5	0
Bi/Ca_1	−0.005	0.005	0.25
Bi/Ca_2	0.0075	0.205	0.25
Bi/Ca_3	0.0075	0.405	0.25
Bi/Ca_4	−0.0175	0.605	0.25
Bi/Ca_5	−0.0175	0.805	0.25
$O\ a_1$	−0.065	0.1	0.25
$O\ a_2$	−0.065	0.5	0.25
$O\ a_3$	−0.065	0.9	0.25
$O\ a_4$	−0.065	0.3	0.25
$O\ a_5$	−0.065	0.7	0.25
$O\ p_1$	0.745	0.054	0.035
$O\ p_2$	0.24	0.046	−0.035
$O\ p_3$	0.265	0.15	−0.035
$O\ p_4$	0.265	0.25	−0.035
$O\ p_5$	0.265	0.35	−0.035

half-doped manganites:[14,16] similar to the 3*d*-sensitive *L*-edge data, the scattering is here due to the anisotropic *p* electronic states on Mn atoms that are electronically and crystallographically equivalent, specifically the Mn atoms sitting in the Jahn-Teller distorted octahedra. These data confirm the presence of distortions of the O octahedra accompanying the orbital ordering, preventing one from differentiating a purely electronic from a purely structural origin of the phase transition.

The *K*-edge data presented in Fig. 4 also strongly support the WC model. A structure based on the WC model was built in order to demonstrate that it can reproduce the scattering of the six *K*-edge RXD spectra. The model has the same symmetries and follows the same displacement directions (not the same displacement amplitudes) occuring in the $La_{0.33}Ca_{0.66}MnO_3$ structure, in the *Pbnm* space group.[4] In this $x=0.66$ system, the WC model was found, and a trend of displacements can be identified when compared to displacements refined at $x=0.5$.[3] We used the same trend for the directions of the atomic displacements and the *Pbnm* space group to generate a WC model within a larger unit cell, at $x=0.8$. Table I gives the atomic positions used; the scheme in Fig. 5 gives the directions of the displacements in the plane of the orbital ordering. The main ingredients are the tilt of the octahedra (displacements of the apical oxygens), the JT distortions (displacements of the planar oxygens), and the cation and Mn displacements tranverse to the orbital ordering propagation vector, in opposite directions for the two halves of the unit cell (see Fig. 5). The resonant scattering factors were calculated as described above, in the $\sigma \rightarrow \sigma$ channel, using the dipolar approximation (i.e., quadrupolar $s \rightarrow d$ transitions were ignored), with this structure having the
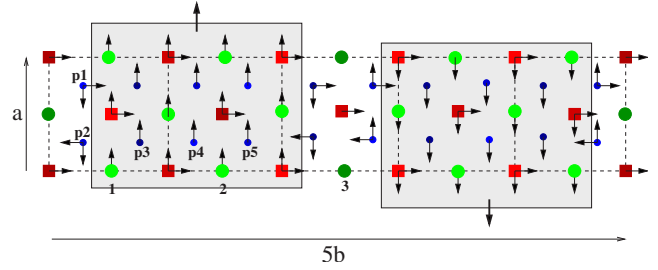

FIG. 5. (Color online) Model of a crystallographic structure for the orbital order phase at $x=0.8$ doping. The arrows indicate the direction of the displacements from the undistorted structure. The displacement pattern is the same as in the structure proposed for $La_{0.33}Ca_{0.66}MnO_3$. The small circles represent planar oxygen atoms. Larger circles are Mn atoms; shaded circles are the Jahn-Teller Mn atoms; the labels corresponds to the atoms listed in Table I. Squares represent the cations.

lattice parameters we found by x-ray diffraction: $a=5.386$, $b=26.720$, and $c=7.449$ Å. Notably, the calculations of the 2δ superstructure reflections reproduce the energy line shapes (Fig. 6). These results are a strong support for the structure because these reflections are extremely sensitive to the pattern of the JT-octahedra.[16] Moreover, the relative intensities of the reflections, and the ratio between on-resonance and off-resonance intensities, are comparable over six orders of magnitude. In Fig. 7 the calculations are instead performed with less distorted JT octahedra in which the planar oxygens atoms undergo the same displacements than those of the undistorted octahedra (the antidistortive order almost vanishes). Comparing with Fig. 6, the main and δ superstructure reflections undergo almost no change. The sensitivity to the displacements is much more pronounced on the 2δ reflections—at the Mn *K*-edge resonance—in intensity and in energy line shapes. The 2δ reflections evidence the changes in the band structure due to the atomic displace-
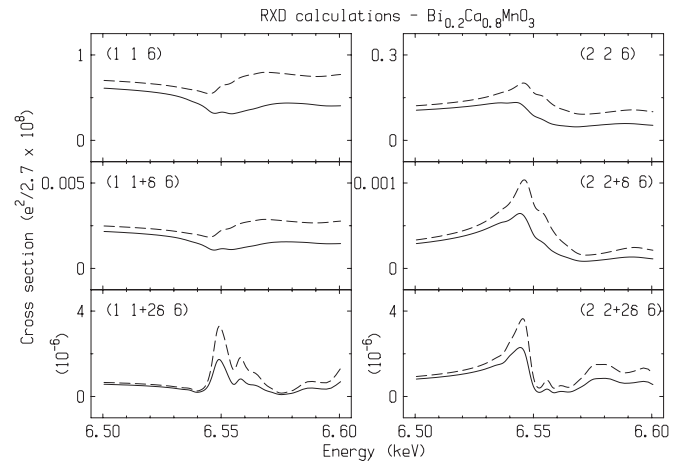

FIG. 6. Calculation of the resonant spectra presented in Fig. 4 using the structure for $Bi_{0.2}Ca_{0.8}MnO_3$ presented in Table I and the FDMNES code (Ref. [17]). The intensities are normalized to the maximum intensity calculated for the (116) reflection. Straight lines are the intensities with self-absorption correction (Ref. [30]), to be compared with Fig. 4; dashed lines are the normalized intensities without the absorption correction.
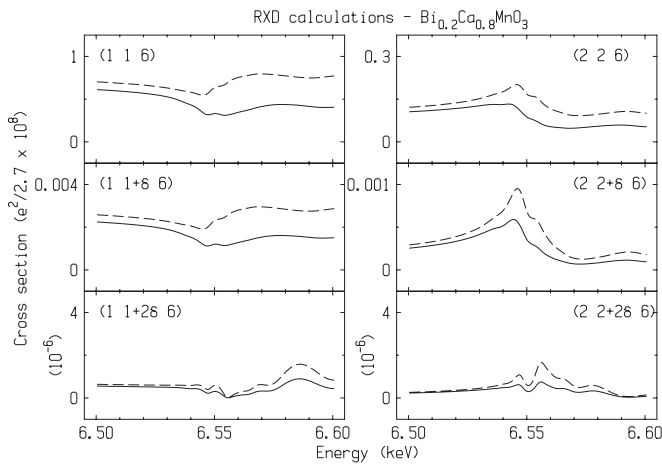
FIG. 7. Illustration of the sensitivity of the resonant spectra to displacements of oxygen atoms. The calculations are performed for the same positions as in Table I, except for the oxygens O $p1$ and O $p2$ which undergo the same displacements as O $p3$, O $p4$ and O $p5$. The positions are (0.765, 0.05, 0.035) for O $p1$ and (0.265, 0.05, −0.035) for O $p2$, with the effect of reducing the distortion of the Jahn-Teller octahedra. Remarkably, only on-resonance scattering of 2δ superstructure reflections is affected, in intensity and in energy line shape.

ments of the JT octahedra. Programs are currently developed in order to use such RXD spectra to constrain the conventional crystallographic methods, in broad analogy with the multiwavelength anomalous method used in biological crystallography. Such code being in the developpment stage,[19] we used a "test and try" method, manually fitting the few crystallographic parameters, only guided by the previous work by Radaelli *et al.* We suggest that the resulting struc-

ture shall be used as input to a standard refinement to neutron or x-ray diffraction data in order to retrieve a more precise structure.

V. CONCLUSION

The L-edge and K-edge experiments combined are the strong evidence for the Wigner-crystal model in the $Bi_xCa_{1-x}MnO_3$ system at high doping. Orbital ordering corresponding to a Wigner-crystal model was directly observed by Mn L-edge diffraction in the $Bi_{0.31}Ca_{0.69}MnO_3$ system with equivalent Mn atoms separated by a distance of $\Lambda/2$ along the orbital ordering direction, ruling out any bi-stripe models. The orbital ordering is accompanied by distortions of the O octahedra. A crystallographic structure with the same propagation vector for equivalent Mn octahedra was obtained after manual fit to the K-edge resonant x-ray diffraction spectra of $Bi_{0.2}Ca_{0.8}MnO_3$. The structure follows the same displacement pattern as the $La_{0.33}Ca_{0.66}MnO_3$ system. We conclude that the Wigner-crystal pattern of electronic order is robust with high hole doping in the $Bi_xCa_{1-x}MnO_3$ system.

[1] S. van Smaalen, P. Daniels, L. Palatinus, and R. K. Kremer, Phys. Rev. B **65**, 060101(R) (2002).

[2] R. J. Goff and J. P. Attfield, Phys. Rev. B **70**, 140404 (2004).

[3] P. G. Radaelli, D. E. Cox, M. Marezio, and S.-W. Cheong, Phys. Rev. B **55**, 3015 (1997).

[4] P. G. Radaelli, D. E. Cox, L. Capogna, S. W. Cheong, and M. Marezio, Phys. Rev. B **59**, 14440 (1999).

[5] P. Benedetti, J. van den Brink, E. Pavarini, A. Vigliante, and P. Wochner, Phys. Rev. B **63**, 060408(R) (2001).

[6] C. W. M. Castleton and M. Altarelli, Phys. Rev. B **62**, 1033 (2000).

[7] S. B. Wilkins, P. D. Spencer, P. D. Hatton, S. P. Collins, M. D. Roper, D. Prabhakaran, and A. T. Boothroyd, Phys. Rev. Lett. **91**, 167205 (2003).

[8] S. S. Dhesi, A. Mirone, C. D. Nadai, P. Ohresser, P. Bencok, N. B. Brookes, P. Reutler, A. Revcolevschi, A. Tagliaferri, O. Toulemonde, and G. Van der Laan, Phys. Rev. Lett. **92**, 056403 (2004).

[9] K. J. Thomas, J. P. Hill, S. Grenier, Y.-J. Kim, P. Abbamonte, L. Venema, A. Rusydi, Y. Tomioka, Y. Tokura, D. F. McMorrow, G. Sawatzky, and M. van Veenendaal, Phys. Rev. Lett. **92**,

237204 (2004).

[10] U. Staub, V. Scagnoli, A. M. Mulders, K. Katsumata, Z. Honda, H. Grimmer, M. Horisberger, and J. M. Tonnerre, Phys. Rev. B **71**, 214421 (2005).

[11] N. Jaouen, J.-M. Tonnerre, G. Kapoujian, P. Taunier, J.-P. Roux, D. Raoux, and F. Sirotti, J. Synchrotron Radiat. **11**, 363 (2004).

[12] M. Benfatto, Y. Joly, and C. R. Natoli, Phys. Rev. Lett. **83**, 636 (1999).

[13] I. S. Elfimov, V. I. Anisimov, and G. A. Sawatzky, Phys. Rev. Lett. **82**, 4264 (1999).

[14] J. García, M. C. Sánchez, J. Blasco, G. Subías, and M. G. Proietti, Inst. Chem. Eng. Symp. Ser. **13**, 3243 (2001).

[15] S. Grenier, A. Toader, J. E. Lorenzo, Y. Joly, B. Grenier, S. Ravy, L. P. Regnault, H. Renevier, J. Y. Henry, J. Jegoudez, and A. Revcolevschi, Phys. Rev. B **65**, 180101(R) (2002).

[16] S. Grenier, J. P. Hill, D. Gibbs, J. K. Thomas, M. v. Zimmermann, C. S. Nelson, Y. Tokura, Y. Tomioka, D. Casa, T. Gog *et al.*, Phys. Rev. B **69**, 134419 (2004).

[17] Y. Joly, Phys. Rev. B **63**, 125120 (2001).

[18] A. Mirone, S. S. Dhesi, and G. van der Laan, Eur. Phys. J. B **53**, 23 (2006).

[19] E. Nazarenko, J. E. Lorenzo, Y. Joly, J. L. Hodeau, D. Mannix, and C. Marin, Phys. Rev. Lett. **97**, 056403 (2006).

[20] Y. Joly, S. Grenier, and J. E. Lorenzo, Phys. Rev. B **68**, 104412 (2003).

[21] J. Herrero-Martin, J. Garcia, G. Subias, J. Blasco, and M. C. Sanchez, Phys. Rev. B **72**, 085106 (2005).

[22] Y. Murakami, H. Kawada, H. Kawata, M. Tanaka, T. Arima, Y. Moritomo, and Y. Tokura, Phys. Rev. Lett. **80**, 1932 (1998).

[23] M. v. Zimmermann, C. S. Nelson, J. P. Hill, D. Gibbs, M. Blume, D. Casa, B. Keimer, Y. Murakami, C.-C. Kao, C. Venkataraman, T. Gog, Y. Tomioka, and Y. Tokura, Phys. Rev. B **64**, 195133 (2001).

[24] J. Rodríguez-Carvajal, M. Hennion, F. Moussa, A. H. Moudden, L. Pinsard, and A. Revcolevschi, Phys. Rev. B **57**, R3189 (1998).

[25] V. I. Anisimov, I. S. Elfimov, M. A. Korotin, and K. Terakura, Phys. Rev. B **55**, 15494 (1997).

[26] W.-G. Yin, D. Volja, and W. Ku, Phys. Rev. Lett. **96**, 116405 (2006).

[27] S. Mori, C. H. Chen, and S.-W. Cheong, Nature (London) **392**, 473 (1998).

[28] R. Wang, J. Gui, Y. Zhu, and A. R. Moodenbaugh, Phys. Rev. B **61**, 11946 (2000).

[29] Y. Murakami, J. P. Hill, D. Gibbs, M. Blume, I. Koyama, M. Tanaka, H. Kawata, H. Arima, Y. Tokura, K. Hirota, and Y. Endoh, Phys. Rev. Lett. **81**, 582 (1998).

[30] $I = I_{calc}/\mu^*$ where $\mu^* = (\mu_{Mn} + 0.2\mu_{Bi} + 0.8\mu_{Ca} + 3\mu_O)/(0.2\mu_{Bi} + 0.8\mu_{Ca} + 3\mu_O)$, the absorption coefficients are calculated using the FDMNES code for the Mn atoms, and the Cromer-Liberman tables for the other atoms.